Comparative Molecular Field Analysis of Hydantoin Binding to the Neuronal Voltage-Dependent Sodium Channel

Milton L. Brown,[†] Congxiang C. Zha,[†] Christopher C. Van Dyke,[§] George B. Brown,[‡] and Wayne J. Brouillette*[,†]

Departments of Chemistry and of Psychiatry and Behavioral Neurobiology, University of Alabama at Birmingham, Birmingham, Alabama 35294, and Tripos, Inc., 1699 South Hanley Road, Suite 303, St. Louis, Missouri 63144

Received September 30, 1998

Comparative molecular field analysis (CoMFA), a 3-D QSAR technique, is widely used to correlate biological activity with observed differences in steric and electrostatic fields. In this study, CoMFA was employed to generate a model, based upon 14 structurally diverse 5-phenylhydantoin analogues, to delineate structural and electrostatic features important for enhanced sodium channel binding. Correlation by partial least squares (PLS) analysis of in vitro sodium channel binding activity (expressed as log IC_{50}) and the CoMFA descriptor column generated a final non-cross-validated model with $R^2 = 0.988$ for the training set. The final CoMFA model explained the data better than a simpler correlation with log *P* ($R^2 = 0.801$) for the same training set. The CoMFA steric and electrostatic maps described two general features that result in enhanced binding to the sodium channel. These include a preferred 5-phenyl ring orientation and a favorable steric effect resulting from the C5-alkyl chain. This model was then utilized to accurately predict literature sodium channel activities for hydantoins **14**−**20**, which were not included in the training set. Finally the hydantoin CoMFA model was used to design the structurally novel α-hydroxy-α-phenylamide **21**. Synthesis and subsequent sodium channel evaluation of compound **21** (predicted $IC_{50} = 9\ \mu M$, actual $IC_{50} = 9\ \mu M$), a good binder to the sodium channel, established that the intact hydantion ring is not necessary for efficient binding to this site. Thus α-hydroxy-α-phenylamides may represent a new class of ligands that bind with increased potency to the sodium channel.

The anticonvulsant diphenylhydantoin (DPH), or phenytoin, binds to the neuronal voltage-sensitive sodium channel (NVSC) at therapeutically relevant concentrations in a frequency- and voltage-dependent manner.[1] These observations are consistent with the selective actions of DPH on hyperactive versus normal neurons.

Our earlier studies[2,3] on hydantoin analogues revealed that, when log *P* is held constant, structural variations lead to dramatic differences in sodium channel binding potency. This observation, when coupled with the reported[4] saturable effects of DPH on sodium channels, suggests that DPH undergoes interaction with a specific site on the NVSC.

Unfortunately, the exact location of this site and structural requirements for optimum binding have not yet been determined. Our previous observation of the strong influence of log *P*, given an appropriate structural type, on the in vitro binding of hydantoins to the NVSC suggests that membrane entry may be required for activity. This observation and the report that changes in intracellular pH affect the activity of DPH on sodium channels are consistent with an intracellular binding site.[5] Given the absence of high-resolution structural data for the NVSC, in the present study we employed comparative molecular field analysis (CoMFA) to help define important 3-dimensional (3-D) properties associated with the optimum binding of hydantoins to this site. CoMFA samples the differences in steric and electrostatic fields surrounding a set of ligands. Numerous successes have been reported using this approach for mapping receptor properties, including studies on central nervous system (CNS) active compounds[6−21] as well as a NVSC study[22] which evaluated the binding of brevetoxins to neurotoxin site 5.

In this study we utilized sodium channel binding data for hydantoin analogues that we previously published,[2] and we additionally synthesized and evaluated the sodium channel binding activities for 5-alkyl-5-phenylhydantoins **5**−**7** to extend the series to include larger log *P* values. Sodium channel binding data for hydantoins **1**−**13** and DPH (Table 1) were used to evaluate correlations with log *P* and derive a CoMFA model. The CoMFA model derived from the training set in Table 3 was then used to predict the sodium channel binding activities of hydantoin analogues **14**−**19** and carbamazepine (**20**) (Table 4) and to design a novel ligand, hydroxyamide **21**.

Methods

Biological Data. The structures and relative sodium channel binding activities for compounds **1**−**13** and DPH, which form the training set, are listed in Table 1. Table 4 describes the structures and sodium channel binding activities of compounds **14**−**21**, which form the test set. In the sodium channel evaluation, the IC_{50}, which represents the micromolar concentration of compound required to displace 50% of specifically bound [^{3}H]batrachotoxinin A 20-α-benzoate ([^{3}H]BTX-B), was determined in an in vitro assay using rat brain cerebral

* Address correspondence to this author.
[†] Department of Chemistry, University of Alabama at Birmingham.
[‡] Department of Psychiatry and Behavioral Neurobiology, University of Alabama at Birmingham.
[§] Tripos, Inc.

10.1021/jm980556l CCC: $18.00
Published on Web 04/08/1999

Table 1. Data from the PLS Cross-Validated Analysis

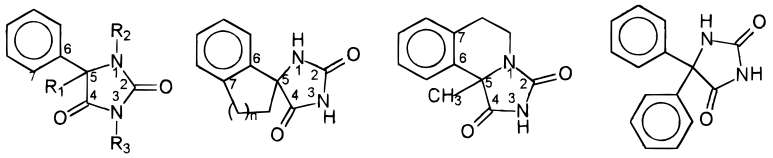

1-8 **9-12** **13** **DPH**

compd	R_1	R_2	R_3	*n*	torsion angle (deg) N1,C5,C6,C7	preliminary model, −log IC_{50} obsd	preliminary model, −log IC_{50} pred	preliminary model, −log IC_{50} res	final model, −log IC_{50} obsd	final model, −log IC_{50} pred	final model, −log IC_{50} res
1	*n*-propyl	H	H		5	−2.21	−2.00	−0.21	−2.21	−2.03	−0.18
2	*n*-butyl	H	H		5	−2.01	−1.91	−0.10	−2.01	−2.03	0.02
3	*n*-butyl	H	methyl		5	−2.45	−1.90	−0.55	−2.45	−2.01	−0.44
4	*n*-pentyl	H	H		5	−1.59	−1.72	0.13	−1.59	−1.67	−0.12
5	*n*-hexyl	H	H		5	−1.11	−1.29	0.18	−1.11	−1.12	0.01
6	*n*-heptyl	H	H		5	−0.70	−1.00	0.30	−0.70	−0.91	0.21
7	*n*-nonyl	H	H		5	−0.70	−0.63	−0.07	−0.70	−0.72	0.02
8a	methyl	ethyl	H		−45	−2.86	−2.91	0.05	−2.86	−2.74	−0.12
8b	methyl	ethyl	H		−57	−2.86	−3.80	0.20			
9a				1	−36	−3.32	−2.88	−0.44	−3.32	−2.54	−0.68
9b				1	−76	−3.32	−2.71	−0.61			
10a				2	−43	−2.93	−2.93	0.00	−2.93	−2.58	0.19
10b				2	−65	−2.93	−2.75	−0.18			
11a				3	−17	−2.40	−2.47	0.07	−2.40	−2.58	0.18
11b				3	−27	−2.40	−2.57	0.17			
11c				3	−44	−2.40	−2.70	0.30			
11d				3	−75	−2.40	−2.57	0.17			
11e				3	−93	−2.40	−2.69	0.29			
11f				3	−63	−2.40	−2.81	0.41			
12a				4	−10	−2.40	−2.24	−0.16			
12b				4	−18	−2.40	−2.37	−0.03	−2.40	−2.28	−0.12
12c				4	−25	−2.40	−2.25	−0.15			
12d				4	−63	−2.40	−2.38	0.02			
12e				4	−73	−2.40	−2.35	−0.05			
13a					−142	−2.40	−2.43	0.03	−2.40	−2.53	0.13
13b					−179	−2.40	−2.45	0.05			
DPH	phenyl	H	H			−1.60	−2.10	0.50	−1.60	−2.20	0.06

Table 2. Cross-Validated PLS Analysis[a]

components	preliminary model[b] *s*	preliminary model[b] R^2	final model[c] *s*	final model[c] R^2
1	0.561	0.301	0.531	0.573
2	0.406	0.648	0.457	0.736
3	0.342	0.762	0.404	0.821
4	0.314	0.808	0.404	0.844
5	0.293	0.840	0.430	0.847

[a] *s*, standard error for the estimate of log IC_{50}; R^2, correlation coefficient or press value = 1.0 − {$\sum$(*Y* predicted − *Y* actual)^2 ÷ (*Y* actual − *Y* mean)^2 }. [b] The preliminary model included single conformations of **1**−**7** and multiple conformations of **8**−**13**. [c] The final model included single conformations of **1**−**7** and a single best fit (smallest residual as determined from the preliminary model) conformer of **8**−**13**. Optimum number of components is 3 with R^2 = 0.821.

cortex synaptoneurosomes. To calculate the IC_{50} value, the percent inhibition at 5−7 concentrations which spanned the IC_{50} value was determined in triplicate. The IC_{50} value was obtained by a Probit analysis of the concentration versus percent binding curve.

Conformational Analysis. All compounds were energy-minimized with the Tripos force field,[23] without solvent, using default bond distances and angles and neglecting electrostatics. The details were previously described.[2] While compounds were synthesized and evaluated as racemic mixtures, for internal consistency the geometries were modeled using only the *R*-configuration at C5. Since 5-phenyl ring orientation for hydantoin analogues has previously been suggested to be important for hydantoin binding to the NVSC,[24] we designated the C5−C6 bond, which rotates the phenyl ring, for conformational searching. Previously reported[2] low-energy conformers of **1**, **2**, **4**, and **8**−**16** were used. To determine the low-energy conformations for **3** and **5**−**7** about the C5−C6 bond, we utilized GRIDSEARCH to rotate N1, C5, C6, and C7 over 360° in 1° increments as previously reported.[2] A similar approach was used for **21**. For carbamezapine (**20**)[33] the conformation reported for the X-ray crystal structure was utilized.

The results for conformational searches on the rotationally restricted 5-phenyl analogues **9**−**13** using the GRIDSEARCH routine were previously described.[2] In a similar fashion, the low-energy conformations of **17** were obtained by incorporating a cyclohexyl side chain in a chair conformation (obtained from the SYBYL fragment library). The atomic charges for all analogues were calculated using AM1 (MOPAC).

Molecular Alignment. All of the compounds in the training set (Table 3) have identical hydantoin ring atoms, and these were used as the basis for an alignment rule (atoms N1, C2, N3, C4, and C5 were fit onto each other). Similarly, for **14**−**19** in the test set, we aligned the hydantoin ring atoms N1, C2, N3, C4, and C5 and the phenyl ring atom C6. The *n*-alkyl groups at C5 for analogues **1**−**7** in the training set and for **14**−**16**, **20**, and **21** in the test set approximated a fully extended conformation following energy minimization, which was arbitrarily selected for this study. For carbamezapine (**20**)[33] the imide carbonyl oxygen and, for one aromatic ring, the two aromatic carbons that are β to the ring N were fit onto the amide carbonyl oxygen and the two aromatic carbons attached to C6 of

Table 3. Sodium Channel Binding Activities for the Training Set Used in the Final Non-Cross-Validated CoMFA Model[a]

compd	R_1	R_2	R_3	*n*	log *P*	Na^+ channel inhibition IC_{50} (μM)	−log IC_{50} obsd	−log IC_{50} pred[i]	−log IC_{50} res
1	*n*-propyl	H	H		1.96[h]	162 [136−193][e]	−2.21[b]	−2.16	−0.05
2	*n*-butyl	H	H		2.46[h]	103 [85−124]	−2.01[b]	−2.09	0.08
3	*n*-butyl	H	methyl		3.01[h]	285 [232−350]	−2.45[b]	−2.39	0.06
4	*n*-pentyl	H	H		2.96[h]	39 [32−47]	−1.59[b]	−1.61	0.02
5	*n*-hexyl	H	H		3.40	13 [9−17]	−1.11[d]	−1.19	0.08
6	*n*-heptyl	H	H		3.96	5 [4−6]	−0.70[d]	−0.72	0.02
7	*n*-nonyl	H	H		4.96	5 [4−6]	−0.70[c]	−0.52	−0.18
8	methyl	ethyl	H		2.02[j]	720	−2.86[c]	−2.93	0.07
9				1	0.96[j]	2112 [2021−2207]	−3.32[k]	−3.32	0.00
10				2	1.46[j]	851 [761−953]	−2.93[k]	−2.82	−0.11
11				3	1.96[j]	251 [225−280]	−2.4[k]	−2.36	−0.04
12				4	2.46[j]	251 [228−277]	−2.4[k]	−2.36	−0.04
13					1.52[j]	250	−2.4[c]	−2.42	0.02
DPH	phenyl	H	H		2.46[g]	40[f]	−1.6	−1.61	0.01

[a] Number of components = 3, $s = 0.099$, $R^2 = 0.988$. [b] Reported IC_{50} value ± 1 standard deviation in ref 3. [c] Reported IC_{50} value in ref 24. [d] The sodium channel value was determined in this study. [e] Numbers in brackets represent ±1 standard deviation. [f] Data taken from ref 1. [g] Log *P* data taken from ref 30. [h] Calculated using parent structure log *P* value in ref 3. [i] Generated from the CoMFA non-cross-validated run (see Methods). [j] Calculated using parent structure log *P* value in ref 2. [k] Reported IC_{50} value in ref 2.

Table 4. Predicted and Actual Sodium Channel Binding Activities for Diverse Analogues Forming the Test Set

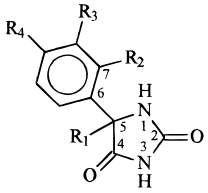

14-17

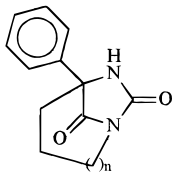

18 (n=2), **19** (n=3)

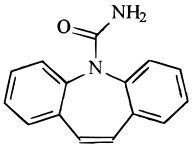

20

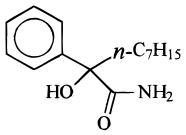

21

compd	R_1	R_2	R_3	R_4	energy (kcal/mol)	torsion angle (deg) N1,C5,C6,C7	log *P*	Na^+ channel inhibition[c] IC_{50} (μM)	−log IC_{50} (μM) obsd	−log IC_{50} (μM) pred[d]	−log IC_{50} (μM) res
14(a)	*n*-butyl	methyl	H	H	10.8	−37	2.96[e]	225 [218−233]	−2.35	−2.27	−0.08
14(b)	*n*-butyl	methyl	H	H	12.4	159	2.96[e]	225 [218−233]	−2.35	−2.37	0.02
15	*n*-butyl	H	methyl	H	8.2	4	2.96[e]	58[c] [57−60]	−1.76	−2.03	0.26
16	*n*-butyl	H	H	methyl			2.96[e]	95 [86−106]	−1.98	−2.03	0.05
17	cyclohexyl	H	H	H			2.96	58 [41−82]	−1.76	−1.89	0.13
18(a)					40.4	86	2.01[b]	700[a]	−2.85	−3.11	0.26
18(b)					39.1	−1	2.01[b]	700[a]	−2.85	−2.92	0.07
19(a)					27.0	−1	2.51[b]	427[a] [376−383]	−2.63	−2.72	0.09
19(b)					26.3		2.51[b]	427[a] [376−383]			
20							2.13[g]	131[f]	−2.12	−2.10	−0.02
21							3.70	9 [7−11]	−0.95	−0.95	0.00

[a] Reported in ref 3. [b] Calculated using parent structure log *P* value in ref 24 and π values in ref 32. [c] Numbers in brackets represent ±1 standard deviation. [d] Data generated from the CoMFA non-cross-validated run (see QSAR Methods). [e] Calculated using parent structure log *P* value in ref 2. [f] Reported in ref 1. [g] Calculated using Clog *P*.

DPH (Figure 4C). The hydroxyamide **21** was aligned such that the OH group was superimposed with N1 and the carboxamide was aligned with C4 and N3.

CoMFA Calculations. CoMFA, using default parameters except where noted, was calculated in the QSAR option of SYBYL 6.4 on a Silicon Graphics Octane computer. The CoMFA grid spacing was 2.0 Å in the *x*, *y*, and *z* directions, and the grid region was automatically generated by the CoMFA routine to encompass all molecules with an extension of 4.0 Å in each direction.

Table 5. Selected Data for New Compounds[a]

compd	isolated yield (%)	mp (°C) (recryst solvent)	^{1}H NMR (DMSO-d_6)[b]	^{13}C NMR (DMSO-d_6)[c]	IR (cm^{-1}) (C=O), KBr
5	59	138−140 [lit. 140−142][d] (ethanol)			
6	21	124−126 (ethanol)	10.91−10.65 (s, 1H, NH), 8.79−8.56 (s, 1H, NH), 7.65−7.15 (m, 5H, Ph), 2.15−1.68 (s, 2H, CH_2), 1.45−0.98 (m, 10H, CH_2), 0.94−0.63 (m, 3H, CH_3)	176.3, 156.5, 139.3, 128.4, 127.7, 125.3, 67.5, 31.1, 28.7, 28.5, 23.3, 22.2, 13.9	1755, 1710
7	95	115−116 (ethanol)	10.98−10.53 (s, 1H, NH), 8.70−8.44 (s, 1H, NH), 8.08−7.87 (m, 1H, Ph), 7.73−7.16 (m, 4H, Ph), 3.09−2.85 (s, 1H, CH), 2.11−1.68 (s, 2H, CH_2), 1.68−1.43 (m, 12H, CH_2), 1.40−1.04 (m, 12H, CH_2), 0.99−0.61 (m, 3H, CH_3)	176.9, 156.1, 139.8, 129.0, 128.2, 125.9, 67.1, 36.3, 28.8, 28.4, 28.4, 28.3, 28.2, 22.8, 21.7, 13.5	1750, 1700
21	100	91−92 (toluene)	7.74−7.43 (m, 2H, Ph), 7.43−7.10 (m, 3H, Ph), 6.62−6.27 (s, 1H, NH), 5.90−5.60 (s, 1H, NH), 3.54−3.17 (s, 1H, OH), 2.30−2.12 (m, 1H, CH), 2.08−1.89 (m, 1H, CH), 1.56−1.08 (m, 10H, CH_2), 0.94−0.59 (m, 3H, CH_3)	177.0, 142.4, 128.5, 127.8, 125.4, 78.8, 39.2, 31.8, 29.7, 29.2, 23.4, 22.6, 14.1	1660

[a] All compounds were also analyzed by (1) GC/MS (EI, 70 eV), giving one peak in the GC and the expected molecular ion peak, and (2) elemental analysis for C, H, N (within ±0.4% of the calculated value). [b] Compound **20** ^{1}H NMR taken in $CDCl_3$. [c] Compound **20** ^{13}C NMR taken in $CDCl_3$. [d] Compound reported in ref 28.

An sp^3 carbon and a charge of +1.0 were used as probes to generate the interaction energies at each lattice point. The default value of 30 kcal/mol was used as the maximum electrostatic and steric energy cutoff.

For the preliminary and final cross-validated CoMFA models (Table 2), the lowest energy conformer for the analogues **1**−**7** was used, which in all cases contained a phenyl ring orientation similar to that found in the X-ray crystal structure[25] of DPH (see Table 1). For compounds **8**−**13**, as a first approach in the preliminary CoMFA model, all low-energy conformations within 5.0 kcal/mol of the global minimum were included, and the single conformer with the smallest cross-validated residual value was selected (Table 1). These single conformers of **8**−**13** were used in both the final cross-validated CoMFA model (Table 2) and the non-cross-validated model (Table 3).

We also used the final non-cross-validated CoMFA model to predict the sodium channel binding activities for all low-energy conformations of the test set compounds **14**−**21** (Table 4).

Partial Least Squares (PLS) Regression Analysis. Cross-validated (preliminary and final models) and non-cross-validated PLS analyses (final model) were performed within the SYBYL/QSAR routine. Cross-validation of the dependent column (log IC_{50}) and the CoMFA column was performed with 2.0 kcal/mol column filtering. Scaled by the CoMFA standard deviation, the final cross-validated analysis generated an optimum number of components equal to 3 and $R^2 = 0.821$ (Table 4). PLS analysis with non-cross-validation, performed with 3 components, gave a standard error of estimate of 0.099, a probability ($R^2 = 0$) equal to 0.000, an F value ($n_1 = 4$, $n_2 = 9$) of 286, and a final $R^2 = 0.988$. The relative steric (0.748) and electrostatic (0.252) contributions to the final model were contoured as the standard deviation multiplied by the coefficient at 80% for favored steric (contoured in green) and favored positive electrostatic (contoured in blue) effects and at 20% for disfavored steric (contoured in yellow) and favored negative electrostatic (contoured in red) effects, as shown in Figure 4.

On the basis of this analysis, the sodium channel binding activities for low-energy conformers of analogues **14**−**20**, from the test set (Table 4), were predicted. The quality of these predictions prompted us to design a structurally unique compound, α-hydroxy-α-phenylamide **21**, which met requirements of the model but did not contain a hydantoin ring. As discussed below, predictions regarding the relatively potent activity for this compound were correct.

Chemistry

The syntheses of analogues **1**−**4**,[3] **8**,[2] **11**,[29] **12**,[29] **13**,[2] **14**−**16**,[2] **17**,[15] and **18**−**19**[3] were previously described. Compounds **5**[28] (59% yield), **9**[27] (31% yield), and **17**[28] (15% yield) were prepared from commercially available hexanophenone, 1-indanone, and cyclohexyl phenyl ketone, respectively, using the Bucherer−Berg approach.[28] Hydantoins **6** and **7** each were prepared in an isolated yield of 95% from commercially available octanophenone and decanophenone, respectively, according to literature methods[26,28] (see Scheme 1).

The synthesis of the 2-hydroxy-2-phenylnonanamide (**21**) was accomplished using a previously reported procedure[26] for the synthesis of 2-hydroxy-2-phenylpropanamide (Scheme 1). Briefly, octanophenone (**22**) was treated under anhydrous conditions with cyanotrimethylsilane to give the cyanotrimethylsilyl ether **23**, and cleavage of the trimethylsilyl group in **23** with 5% HCl gave cyanohydrin **24** in 100% yield. The hydrolysis of **24** with cold concentrated HCl and HCl gas resulted in the precipitation of 2-hydroxy-2-phenylnonanamide (**21**) in 100% yield.

Results and Discussion

Our previous sodium channel SAR studies[3] suggested that log P was one of the parameters important for enhanced binding of hydantoins to the NVSC. We thus estimated the log P values for analogues **5**−**7** and **17**−**20** (Tables 1 and 2) by the approach we employed earlier, using reported experimentally measured log P values for the parent structures, 5-phenylhydantoin (log $P = 0.46$)[30] and 2-hydroxy-2-phenylpropanamide (log $P = 1.2$),[31] to which were added the appropriate π values for the substituents at C5 and N1 to provide the final log P.[32] The π values used were 0.50 for each CH_2 or

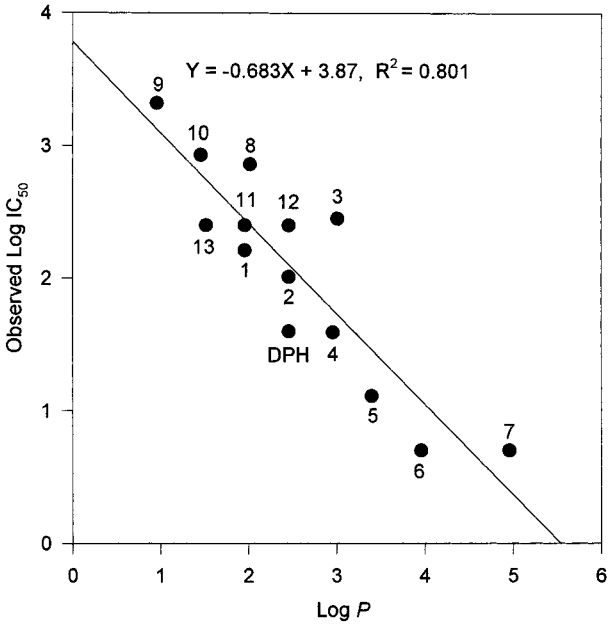

Figure 1. Plot of log *P* versus observed log IC_{50} for the training set.

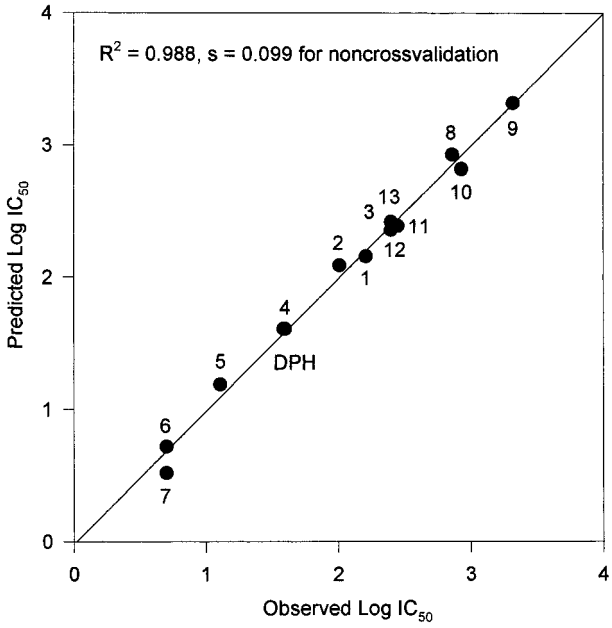

Figure 2. Plot of observed log IC_{50} versus predicted log IC_{50} values for the non-cross-validated CoMFA model in Table 3.

Scheme 1

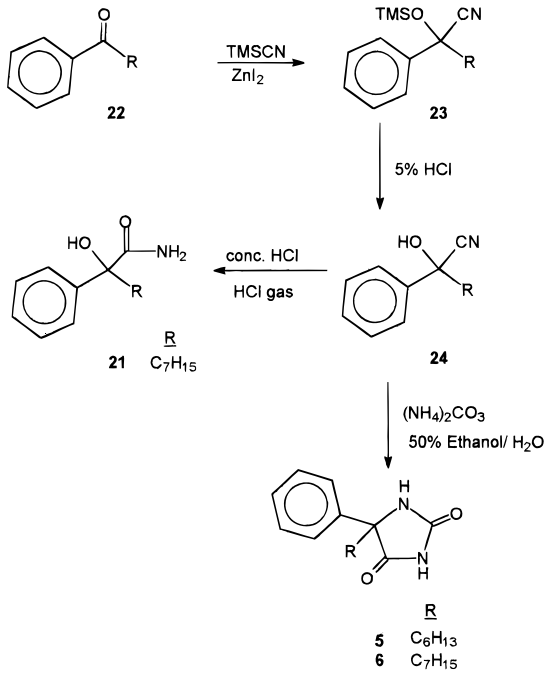

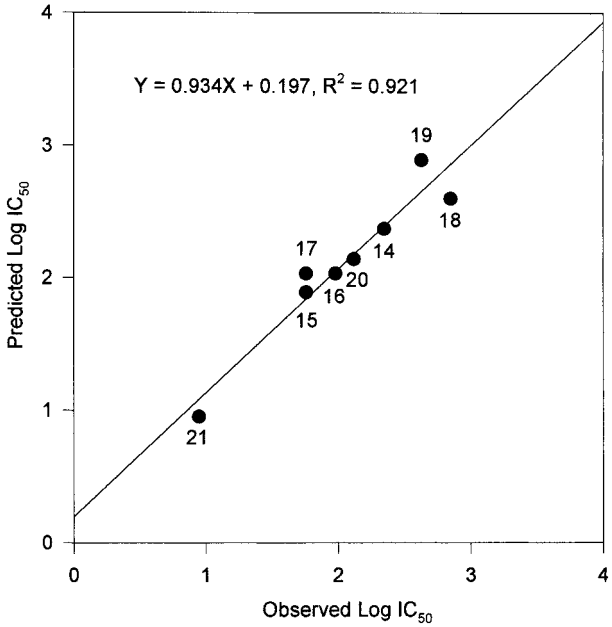

Figure 3. Plot of observed log IC_{50} versus predicted log IC_{50} for the test set in Table 4.

CH_3 in the alkyl chain at C5 and 0.56 for an *N*-CH_3 substitute. For example, the log *P* for hydantoin **8** was calculated as ($\log P_{5\text{-phenylhydantoin}} + \pi_{5\text{-methyl}} + \pi_{\text{N1-methylene}} + \pi_{\text{methyl}}$) = (0.46 + 0.50 + 0.56 + 0.50) = 2.02. Since the ring closure of **8** provides the bicyclic hydantoin **13**, the log *P* of **13** was calculated as ($\log P_{\mathbf{8}} + \pi_{\text{ring closure}}$) = 2.02 + (−0.50) = 1.52. The log *P* values for previously reported compounds[2] were similarly calculated.

The correlation of log *P* versus sodium channel binding (log IC_{50}) for **1**−**13** and DPH, shown in Figure 1, resulted in a better quality model than a previously reported[2] log *P* model, which used fewer compounds and spanned a smaller log *P* range. However, comparisons within the present model of hydantoins with the same log *P* and different structures often show very different binding affinities to the NVSC (e.g., **3** vs **4**). Thus a number of points deviate from the regression line. Note that, since the most effective inhibitors begin to approach unfavorable log *P* values, compounds in the lower right quadrant which deviate to the left of the correlation line are most likely to have clinical relevance (high potency and moderate log *P*). We thus were encouraged to use CoMFA to investigate the differences in structural and electrostatic features of these analogues in an effort to formulate a better model.

The sodium channel binding affinities and lipophilicities for the CoMFA training set are presented in Table 3. PLS correlation of in vitro sodium channel binding, expressed as −log IC_{50}, and CoMFA descriptors generated a CoMFA model with R^2 = 0.988 for the training set (see Table 3). Furthermore, the CoMFA

model provided a better correlation than that for the log *P* model ($R^2 = 0.801$) for the same data set.

Investigations of the CoMFA steric map revealed that *n*-alkyl substitution at the C5 position appears to be required for tight binding to the hydantoin site. The contour map in Figure 4 reveals a favorable steric volume near the 5-alkyl side chain with an optimum length of 6−7 carbons (further increases gave no enhancement in binding). For hydantoins **8**−**12**, which contain conformationally restricted phenyl rings, the CoMFA model supports the conclusion that 5-phenyl ring orientation is important for binding.[2] Compounds **9** and **10** have 5-phenyl rings restrained to spatial arrangements that occupy unfavorable steric regions of the model and are therefore less active sodium channel binders. Analogues **11** and **12** have greater phenyl ring flexibility and can adopt low-energy conformations that allow for occupation of more favorable steric regions, consistent with significantly increased binding potency as compared to hydantions **9** and **10**. Figure 4A, which contains highly active analogue **7** (orange) and the weakly active hydantoin **9** (green) within the electrostatic and steric CoMFA fields, respectively, illustrates the effects of proper 5-phenyl ring conformation on binding.

An important property of a QSAR model is the ability to accurately predict the relative binding potencies of new analogues. The predictive ability of the CoMFA model described here was first evaluated by calculating activities of previously published monocyclic hydantoins **14**−**16**,[2] hydantoin **17**, and bicyclic hydantoins **18** and **19**.[3] As shown in Table 4, calculations agreed remarkably well with the experimental results. Hydantoins **14**−**16** (Table 4), which have essentially identical log *P* values, were designed to confirm the importance of 5-phenyl ring orientation independent of changes in log *P*.[2] Compound **14** contains high-energy phenyl ring rotamers that are significantly less populated as compared to the less restricted analogues **15** and **16**. As shown in Figure 4B, the phenyl ring of the lowest energy conformer of **14**(a) does not occupy a sterically favored region of space. This is consistent with a predicted and observed binding affinity for **14**(a) that is 4 times less potent than that of **15** (for both a and b conformations of the methyl group, Table 4) and twice as inactive as **16**.

The substitution of a *p*-methyl group in compound **16** does not appreciably alter phenyl ring orientation relative to a nonsubstituted phenyl ring. Consistently, compound **16** ($IC_{50} = 95\ \mu M$) exhibited essentially the same binding potency as **2** ($IC_{50} = 103\ \mu M$), which has the same size *n*-butyl side chain. Comparisons of analogue **16** (same log *P* and phenyl ring torsion angle) with hydantoin **4** suggest that, given the same log *P* and phenyl torsion angle, longer alkyl side chains provide better sodium channel binders. Further, *m*-methyl may be favored over *p*-methyl substitutions, as suggested by the moderately increased binding potency of **15** as compared to **16** (same log *P* and phenyl ring torsion).

Compound **17** was designed to test the influence of a more bulky, cyclic alkyl group in the 5-alkyl region. Interestingly, the sodium channel binding potency of compound **17** was correctly predicted by the CoMFA model (observed $IC_{50} = 58\ \mu M$). Thus even cyclic groups in the 5-alkyl region favor sodium channel binding.

Additionally, the potential utility of this CoMFA model for designing new, potent sodium channel binders was evaluated. Using the CoMFA model, the α-hydroxy-α-phenylamide **21** was designed as a new structural class that met all major requirements of the model yet did not contain the hydantoin ring. Compound **21** contains, like **1**−**7**, a relatively unrestricted phenyl ring and a seven-carbon 5-alkyl side chain. The success of this compound as a potent sodium channel binder ($IC_{50} = 9\ \mu M$) and the accuracy of prediction by the CoMFA model validate the alignment rule and reveal that the intact hydantion ring is not required for good sodium channel binding activity.

We also used this CoMFA model to predict the activity of carbamazepine (**20**), one of the most common anticonvulsants known to act on the sodium channel, to further verify the value of the model. The alignment used for **20** was previously described and is illustrated in Figure 4C. Despite significant structural differences between carbamazepine and the hydantoins, the model accurately predicts the sodium channel binding activity (actual log $IC_{50} = 2.12$, predicted log $IC_{50} = 2.10$) for **20**.

In conclusion, the CoMFA model in this study was predictive of sodium channel binding affinities for a number of structurally diverse hydantoins, as well as carbamazepine, that were not included in the training set. Furthermore, the CoMFA model was shown to have potential utility for designing new agents in that a structurally novel α-hydroxy-α-phenylamide was also accurately predicted. Thus this CoMFA model, based only on electrostatic and steric effects, may prove useful for designing new and more potent sodium channel-directed agents.

Experimental Section

Melting points were recorded on an Electrothermal melting apparatus and are uncorrected. IR spectra were recorded on Beckman Acculab 6 and Nicolet IR/42 spectrometers, and elemental analyses were performed by Atlantic Microlabs of Norcross, GA. ^1H and ^{13}C NMR spectra were recorded on GE 300 MHz FT and Bruker 300 FT MHz NMR spectrometers in DMSO-d_6 (for hydantoins) and $CDCl_3$ (for all other compounds) at ambient temperature and referenced internally to tetramethylsilane (TMS). The GC/MS analyses were performed on a Hewlett-Packard 5885 GC/MS. Statistics and graphs were generated with SigmaStat (version 1.02a) and Sigma Plot (version 1.0) for Windows from Jandel, Inc. [^3H]Batrachotoxinin A 20-α-benzoate ([^3H]BTX-B) with a specific activity of 30 Ci/mol was obtained from New England Nuclear (Boston, MA).

5-Heptyl-5-phenylhydantoin (6). A mixture containing octanophenone (**22**) (1.5 g, 7.5 mmol), cyanontrimethylsilane (TMSCN) (0.70 g, 7.5 mmol), and ZnI_2 (5−10 mg) was stirred at room temperature under a N_2 atmosphere. The reaction progress was monitored by the disappearance of the C═O stretching peak (1670 cm^{-1}) in the IR spectrum of the reaction mixture. After 2 h this peak was absent, indicating complete conversion to give 2-(trimethylsilyloxy)-2-phenylnonanecarbonitrile (**23**). The TMS ether **23** was hydrolyzed to the cyanohydrin **24** by adding ether (10 mL) and 15% HCl (10 mL), and the resulting mixture was stirred vigorously for 1 h. The acidic layer was washed with ether (3 × 20 mL). The extracts were combined and evaporated to give cyanohydrin **24** (1.8 g, 100%): IR (neat) 3400 (OH), 2250 (CN) cm^{-1}. The cyanohydrin **24** was converted to hydantoin by a previously reported literature procedure for similar compounds.[2] Using this pro-

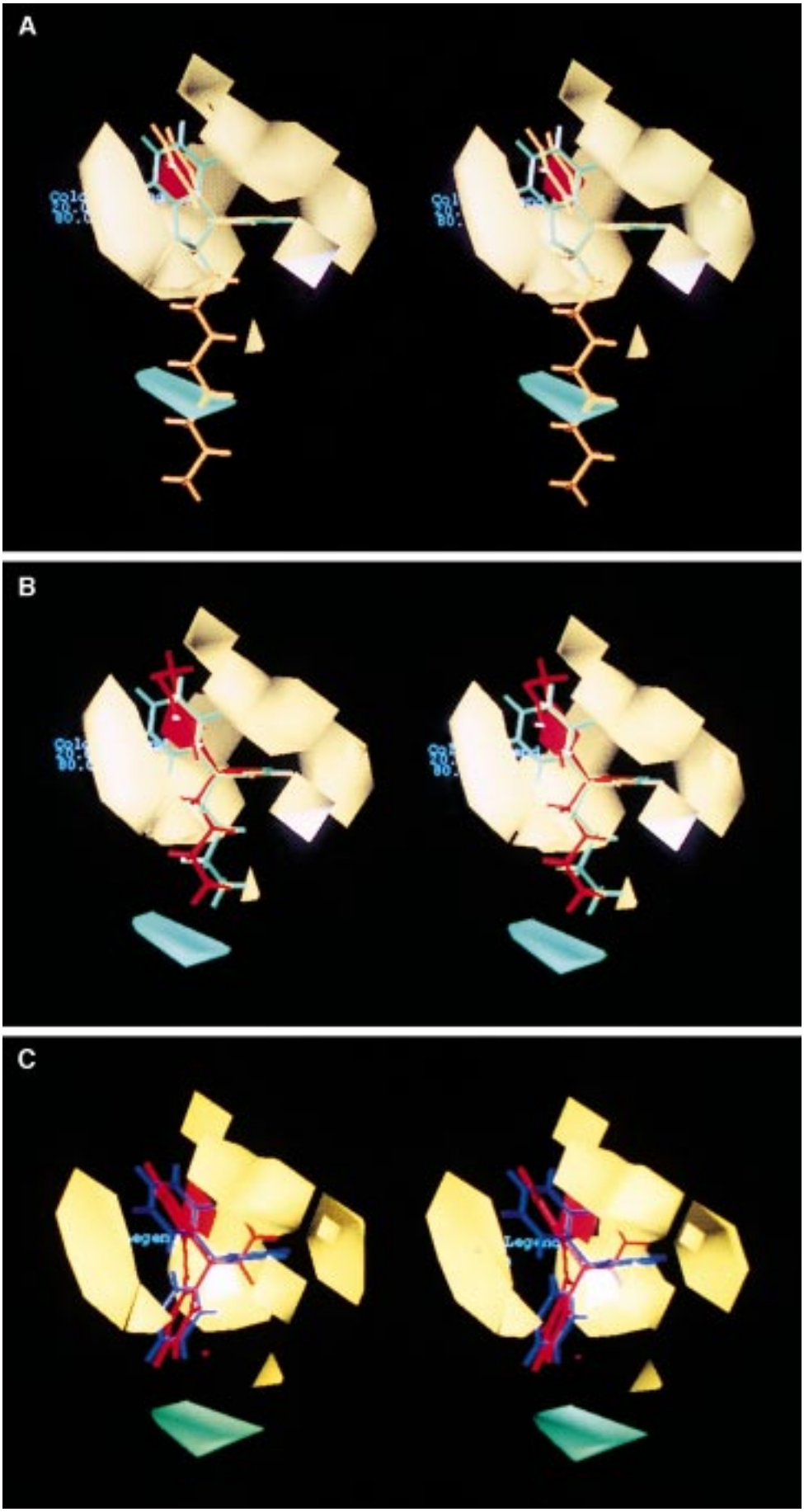

Figure 4. Stereoviews (relaxed) of the electrostatic and steric CoMFA fields for selected compounds. For electrostatic contours increased binding results from placing more positive (+) charge near blue and negative (−) charge near red. For steric contours increased binding results from placing more bulk near green and less bulk near yellow. A. Active analogue **7** (orange) and inactive analogue **9** (green). B. Active analogue **15** (red) and less active analogue **14** (blue). C. Carbamazepine (**20**; red) and DPH (blue).

cedure, cyanohydrin **24** (1.8 g, 9.0 mmol) and $(NH_4)_2CO_3$ (3.6 g, 3.6 mmol) were dissolved in 50% ethanol (30 mL) while stirring under a N_2 atmosphere. The mixture was heated slowly between 40 and 60 °C for 12 h. The basic mixture was evaporated to one-half volume and cooled to room temperature. The precipitate was filtered and recrystallized from hot ethanol to give **6** (0.50 g, 21%): mp 124−126 °C; IR (KBr) 1710, 1755 (C═O), 3200 (NH) cm^{-1}.

5-Nonyl-5-phenylhydantoin (7). To a stirring solution of 50% ethanol (50 mL) were added decanophenone (3.0 g, 13 mmol), KCN (1.7 g, 26 mmol), and $(NH_4)_2CO_3$ (5.9 g, 52 mmol). The solution was warmed to 50−65 °C for 12 h. The precipitate was filtered, and the filtrate was acidified (pH 2) using concentrated HCl. The resulting solid was filtered, and the filtrate was made basic (pH 8) using 3% KOH. This was concentrated to one-half volume and filtered again. The combined solids were recrystallized from hot ethanol to give pure **7** (3.7 g, 95% yield): mp 115−116 °C; IR (KBr) 1700, 1750 (C═O), 3200 (NH) cm^{-1}.

2-Hydroxy-2-phenylnonanamide (21). The cyanohydrin **24** was prepared as described in the synthesis of **6**, except that octanophenone (**22**) (4.1 g, 2.0 mmol), TMSCN (2.0 g, 2.0 mmol), ZnI_2 (5−10 mg), ether (20 mL), and 5% HCl (10 mL) were used. Cyanohydrin **24** was added to cold concentrated HCl (10 mL) and saturated with HCl gas while stirring. After 4 h a precipitate began to form, and the mixture was then allowed to stand overnight without stirring. The solid was filtered, washed on the filter with cold water (3 × 50 mL), and recrystallized from hot toluene to give pure **21** (5.3 g, 100%): mp 91−92 °C.

Sodium Channel Binding Assay. The details for the sodium channel binding assay were reported in a previous paper.[32] Synaptoneurosomes were prepared from rat cerebral cortex as follows. The cerebral cortex (gray matter) was obtained by removing the white matter and other subcortical structures. An incubation buffer was prepared which contained 130 mM choline chloride, 50 mM HEPES, 5.5 mM glucose, 0.8 mM $MgSO_4$, and 5.4 mM KCl, adjusted to pH 7.4 using Tris base. The tissue (about 1 g) was then homogenized in 2 mL of incubation buffer using 10 full strokes of a glass−glass homogenizer. The tissue preparation was transferred to a centrifuge tube, the homogenizer was rinsed with 3 mL of the incubation buffer, and the rinse was combined with the preparation. The preparation was then centrifuged at 1000*g* for 15 min at 4 °C. The pellet was resuspended in a total volume of 20 mL of the incubation buffer and transferred to a 50-mL homogenizer. Three full strokes were used to homogenize the tissue. The suspension was gently filtered through three layers of 160-μm nylon mesh and then through a Whatman #4 filter paper using house vacuum. The filtrate was centrifuged at 1000*g* for 30 min at 4° C. The pellet was resuspended with 5 mL of isotonic sucrose solution, which contained 10 mM NaH_2PO_4 and 0.32 mM sucrose at pH 7.4 (Tris base). Additional isotonic solution was added as needed to obtain an absorbance of 1 at 280 nm. The isotonic suspension was stored in a freezer for up to 3 months at −70 °C until needed. Prior to the binding assay the tissue was thawed, the suspension was centrifuged at 1000*g* for 20 min at 4 °C, and the pellet was resuspended in the HEPES incubation buffer (using the same volume as the isotonic buffer used to store the tissue).

For the sodium channel binding assay, synaptoneurosomes (∼1 mg of protein) from rat cerebral cortex were incubated for 40 min at 25 °C with the test compound (seven different concentrations spanning the IC_{50}) in a total volume of 320 μL containing 10 nM [^{3}H]BTX-B (specific activity of 30 Ci/mol) and 50 μg/mL scorpion venom. Incubations were terminated by dilution with ice-cold buffer and filtration through a Whatman GF/C filter paper, and the filters were washed four times with ice-cold buffer. Filters were counted in a Beckmann scintillation counter. Specific binding was determined by subtracting the nonspecific binding, which was measured in the presence of 300 μM veratridine, from the total binding of [^{3}H]BTX-B. Each data point used for generating the IC_{50} curve was the mean of triplicate experiments, and each experiment included a control tube containing 40 μM DPH. The IC_{50} values were determined from a Probit analysis of the dose−response curve and excluded doses producing less than 10% or greater than 90% inhibition.

Acknowledgment. This work was completed in partial fulfillment of the requirements for the Ph.D. degree in Organic Chemistry by M.L.B. This work was supported in part by financial support from the Patricia Robert Harris Fellowship, the National Consortium for Educational Access, the UAB Comprehensive Minority Faculty Development Program, and the UAB Department of Chemistry. We also thank Ms. Bereaval Webb, an Alabama Alliance for Minority Participation Summer Intern, for technical support.

References

(1) Willow, M.; Catterall, W. A. Inhibition of Binding of [^{3}H]-Batrachotoxinin A 20-α-Benzoate to Sodium Channels by the Anticonvulsant Drugs Diphenylhydantoin and Carbamazepine. *Mol. Pharmacol.* **1982**, *22*, 627−635.

(2) Brown, M. L.; Brown, G. B.; Brouillette, W. J. Effects of Log P and Phenyl Ring Conformation on the Binding of 5-Phenylhydantoins to the Voltage-Dependent Sodium Channel. *J. Med. Chem.* **1997**, *40*, 602−607.

(3) Brouillette, W. J.; Jestkov, V. P.; Brown, M. L.; Aktar, M. S.; Delorey, T. M.; Brown, G. B. Bicyclic Hydantoins with Bridgehead Nitrogen. Comparison of Anticonvulsant Activities with Binding to the Neuronal Voltage-Dependent Sodium Channel. *J. Med. Chem.* **1994**, *37*, 3289−3293.

(4) Francis, J.; Burnham, W. M. [^{3}H]Phenytoin Identifies a Novel Anticonvulsant-Binding Domain on Voltage-Dependent Sodium Channels. *Mol. Pharmacol.* **1992**, *42*, 1097−1103.

(5) Barber, M. J.; Starmer, C. F.; Grant, A. O. Blockade of Cardiac Sodium Channels by Amitriptyline and Diphenylhydantoin. Evidence for Two Use-dependent Binding Sites. *Cir. Res.* **1991**, *69*, 677−696.

(6) Greco, G.; Novellino, C. S.; Vittora, A. Comparative Molecular Field Analysis on a Set of Muscurinic Agents. *QSAR* **1991**, *10*, 289−299.

(7) Kim, K. H.; Greco, G.; Novellino, E.; Silipa, C.; Vittoria, A. Use of the Hydrogen Bond Potential Function in a Comparative Molecular Field Analysis (CoMFA) on a Set of Benzodiazepines. *J. Comput.-Aided Mol. Des.* **1993**, *7*, 263−280.

(8) Giovanni, G.; Ettore, N.; Fiorini, I.; Nacci, B.; Campiani, G.; Ciani, S. M.; Garofalo, A.; Bernasconii, P.; Mennini, T. Comparative Molecular Field Analysis Model for 6-Arylpyrrolo[2,1-d][1,5]-Benzothiazepines Binding Selectively to the Mitochondrial Benzodiazepine Receptor. *J. Med. Chem.* **1994**, *37*, 4100−4108.

(9) Wong, G.; Koehler, K. F.; Skolnick, P.; Gu, Z.-Q.; Ananthan, P.; Schönholzer, W.; Hyunkeler, W.; Zhang, W.; Cook, M. Synthetic and Computer-Assisted Analysis of the Structural Requirements for Selective, High-Affinity Ligand Binding to Diazepam-Insensitive Benzodiazepine Receptors. *J. Med. Chem.* **1993**, *36*, 1820−1830.

(10) Andre, M. M.; Charifson, P. S.; Constance, E. O.; Kula, N. S.; McPhail, A. T.; Baldessarini, R. J.; Booth, R. G.; Wyrick, S. D. Conformational Analysis, Pharmacophore Identification, and Comparative Molecular Field Analysis of Ligands for the Neuromodulatory δ_3 Receptor. *J. Med. Chem.* **1994**, *37*, 4109−4117.

(11) Ablordeppy, S. Y.; El-Ashmaway, M. B.; Glennon, R. A. Analysis of the Structure Activity Relationships of Sigma Ligands. *Med. Chem. Res.* **1991**, *1*, 425−438.

(12) Thomas, B. F.; Compton, B. R. M.; Semus, S. F. Modeling the Cannabinoid Receptor: A Three-Dimensional Quantative Structure Activity Analysis. *Mol. Pharmacol.* **1991**, *40*, 656−661.

(13) Semus, S. F. A Computer Graphic Investigation into the Structural Requirements for Interaction with the Putative Cannabinoid Receptor Site. *Med. Chem. Res.* **1991**, *1*, 454−460.

(14) Chen, J. M.; Sheldon, A. Structure−Function Correlations for Calcium Binding and Calcium Channel Activities Based on 3-Dimensional Models of Human Annexins I, II, III, V, VII. *Biomol. Struct. Dynam.* **1993**, *10*, 1067−1089.

(15) Rustici, M.; Bracci, L.; Lozzi, P.; Nari, P.; Santucci, A.; Sodani, P.; Spreafico, A.; Niccolai, N. A Model of the Rabies Virus Glycoprotein Active Site. *Biopolymers* **1993**, *33*, 961−969.

(16) Nordvall, G.; Hacksell, U. Binding Site Modeling of the Muscarinic M1 Receptor: A Combination of Homology-Based and Indirect Approaches. *J. Med. Chem.* **1993**, *36*, 967−976.
(17) Caroll, F. I.; Mascrella, S. W.; Kuzemko, M. A.; Goa, Y. G.; Abraham, P.; Lewin, A. H.; Boja, J. W.; Kuhar, M. J. Synthesis, Ligand-Binding and QSAR (CoMFA and Classical) Study of 3β-(3′-Substituted Phenyl), 3β-(4′-Substituted Phenyl), 3β-(3′,4′-Disubstituted Phenyl)tropane-2β-Carboxylic Acid Methyl-Esters. *J. Med. Chem.* **1994**, *37*, 2865−2873.
(18) Agarwal, A.; Taylor, E. W. 3-D QSAR for Intrinsic Activity of 5-HT_{1A} Receptor Ligands by the Method of Comparative Molecular Field Analysis. *J. Comput. Chem.* **1993**, *14*, 237−245.
(19) Langer, T.; Wermuth, C. G. Inhibitors of Prolyl Endopeptidase: Characterization of the Pharmacophoric Pattern Using Conformational Analysis and 3D-QSAR. *J. Comput.-Aided Mol. Des.* **1993**, *7*, 253−262.
(20) Allen, M. S.; LaLoggia, A. J.; Dorn, M. J.; Constantino, G.; Hagen, T. J.; Koehler, K. F.; Skolnick, P.; Cook, J. M. Predictive Binding of □-Carboline Inverse Agonist and Antagonists via the CoMFA/GOLPE Approach. *J. Med. Chem.* **1992**, *35*, 4001−4010.
(21) Calder, J. A.; Wyatt, J. A.; Frenkel, D. A.; Casida, J. E. CoMFA Validation of the Superposition of Six Classes of Compounds Which Block GABA Receptors Non-Competitively. *J. Comput.-Aided Mol. Des.* **1993**, *7*, 45−60.
(22) Rein, K. S.; Baden, D. G.; Gawley, R. E. Conformational Analysis of the Sodium Channel Modulator, Brevetoxin A. Comparison with Brevetoxin B Conformations, and a Hypothesis About the Common Pharmacophore of the "Site 5" Toxins. *J. Org. Chem.* **1994**, *59*, 2101−2106.
(23) Clark, M. D.; Cramer, R. D., III; Opdenbosch, N. V. Validation of the General Purpose Tripos 5.2 Force Field. *J. Comput. Chem.* **1989**, *10*, 982−1012.
(24) Brouillette, W. J.; Brown, G. B.; Delorey, T. M.; Liang, G. Sodium Channel Binding and Anticonvulsant Activities of Hydantoins Containing Conformationally Constrained 5-Phenyl Substituents. *J. Pharm. Sci.* **1990**, *79*, 871−874.
(25) Camerman, A.; Camerman, N. The Stereochemical Basis of Anticonvulsant Drug Action. I. The Crystal and Molecular Structure of Diphenylhydantoin, a Noncentrosymmetric Structure Solved by Centric Symbolic Addition. *Acta Crystallogr.* **1971**, *B27*, 2205−2211.
(26) Grunewald, G. L.; Brouillette, W. J.; Finney, J. Synthesis of α-Hydroxyamides via the Cyanosilylation of Aromatic Ketones. *Tetrahedron Lett.* **1980**, *21*, 1219−1220.
(27) Sarges, R.; Schnur, R. C.; Belletire, J. L.; Peterson, M. J. Spiro Hydantoin Aldose Reductase Inhibitors. *J. Med. Chem.* **1988**, *31*, 230−243.
(28) Novelli, A.; Lugones, Z. M.; Velasco, P. Hydantoins III. Chemical Constitution and Hypnotic Action. *Anales Asoc. Quim. Argentina* **1942**, *30*, 225−231.
(29) Huisgen, R.; Ugi, I. Polycyclische Systeme mit Heteroatomen. *Liebigs Ann. Chem.* **1957**, *610*, 57−66.
(30) Lien, E. Structure−Activity Correlations for Anticonvulsant Drugs. *J. Med. Chem.* **1970**, *13*, 1189−1191.
(31) Hernandez-Gallegos, Z.; Lehmann, P. A. F. Partition Coefficients of Three New Anticonvulsants. *J. Pharm. Sci.* **1990**, *79*, 1032−1033.
(32) Brouillette, W. J.; Brown, G. B.; Delorey, T. M.; Shirali, S. S.; Grunewald, G. L. Anticonvulsant Activities of Phenyl-Substituted Bicyclic 2,4-Oxazolidinediones and Monocyclic Models. Comparison with Binding to the Neuronal Voltage-Dependent Sodium Channel. *J. Med. Chem.* **1988**, *31*, 2218−2221.
(33) Lowes, M. M. J.; Caira, M. R.; Lötter, A. P.; Van Der Watt, J. G. Physicochemical Properties and X-ray Structural Studies of the Trigonal Polymorph of Carbamazepine. *J. Pharm. Sci.* **1987**, *76*, 744−752.
(34) Camerman, A.; Camerman, N. Stereochemical Basis of Anticonvulsant Drug Action II. Molecular Structure of Diazepam. *J. Am. Chem. Soc.* **1972**, *94*, 268−272.
(35) Hanson, A. W.; Röhrl, M. The Crystal Structure of Lidocaine Hydrochloride Monohydrate. *Acta Crystallogr.* **1972**, *B28*, 3567−3571.
(36) Zimányi, I.; Weiss, S. R. B.; Lajtha, A.; Post, R. M.; Maarten, E. A. R. Evidence for a Common Site of Action of Lidocaine and Carbamazepine in Voltage-Dependent Sodium Channels. *Eur. J. Pharmacol.* **1989**, *167*, 419−422.
(37) Postma, S. W.; Catterall, W. A. Inhibition of Binding of ^{3}H-Batrachotoxin A 20-□-Benzoate to Sodium Channels by Local Anesthetics. *Mol. Pharmacol.* **1984**, *25*, 219−227.

JM980556L